17th World Conference on Earthquake Engineering, 17WCEE
Sendai, Japan - September 13th to 18th 2020

Estimation of S-wave Velocity Structure Around the Seismic Isolated Hospital in Aso Area and the Strong Ground Motion During Kumamoto Earthquake

T. Inubushi[(1)], T. Enomoto[(2)], T. Horikago[(3)],

[(1)] Lecture, Kindai University, inubushi@arch.kindai.ac.jp
[(2)] Professor, Kanagawa University, enomot01@kanagawa-u.ac.jp
[(3)] Graduate student, Kanagawa University, r201504449zy@jindai.jp

Abstract

During the Kumamoto earthquake that occurred in April 2016, the ground motion with the seismic intensity of upper 6 was observed in Aso City, Kumamoto Prefecture, Japan. The orbit of the seismic isolation layer at the hospital near the Aso station recorded the maximum displacement of 0.46 m, which exceeded the design expectation; however, the structure was not severely damaged. This displacement value is the largest in the history of earthquake response observations in Japan. However, the response displacement of the hospital model using the strong motion recorded at K-NET Ichinomiya (KMM004), approximately 4.0 km to the east of the hospital, exceeded 1.0 m, and was markedly different from the orbit record; therefore, it is essential to elucidate the cause.

In this study, we analyzed the cause by focusing on the S-wave velocity structure of the ground. We conducted a microtremor array observation in the range of approximately 3 × 7 km centered at the hospital and created the predominant period distribution map. In addition, we estimated the S-wave velocity structure and created the one-dimensional soil structure model in the vicinity of the hospital and K-NET Ichinomiya. Then, we calculated the strong motion at the engineering bedrock by pulling back the observation record of K-NET Ichinomiya at the ground surface position. Next, we estimated the ground motion at the site of the hospital by conducting response analysis using the soil structure model in the vicinity of the hospital, and by pulling up the ground motion. In this analysis, we set the soil mass using past survey results and used the nonlinear characteristics defined in the Japanese Building Standards Law Notice.

It was determined that the predominant periods of the surface strata were not considerably different at both points. However, a significant difference was observed in the deep ground considering the deep strata. The maximum displacement of the hospital evaluated from the response spectrum of estimated ground motion corresponded relatively well with the observation displacement of the orbit record.

Keywords: Kumamoto earthquake, seismic isolation, S-wave velocity structure, microtremor array observation

1. Introduction

During the Kumamoto earthquake that occurred in Japan in 2016, the ground motion with the maximum seismic intensity of 7 was continuously observed in the Mashiki town for a short period of time (4/14: foreshock, 4/16: main shock). At the time of the earthquake, there were 24 seismic isolation buildings in the Kumamoto Prefecture, including those under construction. However, no severe damage occurred, except for the design failure; the buildings demonstrated seismic isolation effects [1]. A seismometer was not installed at the seismic isolated hospital near the Aso station in Aso City (Fig. 1), where the seismic intensity of upper 6 was observed; however, a scribing-type displacement meter was installed, and the isolation layer displacement with one-side amplitude of 0.46 m and both amplitudes of 0.9 m were obtained [1]. This value exceeded the assumption of structural design and was the largest in the history of observation in Japan; however, the function of the hospital was maintained, and it was possible to use it as a disaster base. There is a strong ground motion seismograph point, K-NET Ichinomiya (KMM004), approximately 4.0 km to the east of this hospital. On the basis of the numerical simulation of the seismic isolated hospital model using the current record value, the maximum response displacement of the seismic isolation layer exceeds 1.0 m with one-side amplitude, which is significantly different from the scribble record (Fig. 2); thus, the elucidation of the cause is an important issue [2].

Therefore, in this study, we focus on the soil structure and analyze the cause. First, we conduct the microtremor array observation in the vicinity of the seismic isolated hospital and KMM004 and investigate the predominant period distribution of the ground. In addition, we estimate the one-dimensional S-wave velocity structure in the vicinity of the hospital and near KMM004. Next, we create a one-dimensional soil structure model at both points and estimate the ground motion at the hospital using the observation records at KMM004.

Fig. 1 – Location of Aso City

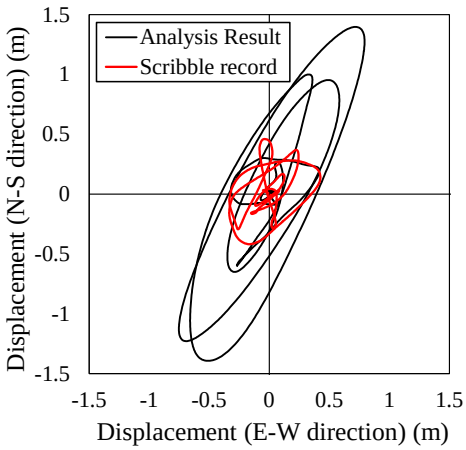

Fig. 2 – Scribble record and seismic response analysis result

2. Outline of seismic isolation hospital and seismic observation record at KMM004

Fig. 3 shows the entire site of the seismic isolated hospital, and Fig. 4 shows the exterior of the building. The central clinic has two floors above ground; the ward has four floors above ground and a penthouse. The superstructure of both buildings is an RC-framed structure with earthquake-resistant walls. The first and second floors are connected to both buildings. Two types of isolation members are used: lead rubber bearing (φ700 mm) and natural rubber bearing (φ700 mm). The horizontal clearance is more than 0.50 m, and the allowable displacement of design for the seismic isolation layer is 0.35 m, which is equivalent to 250% shear strain. The equivalent period of the seismic isolated building at the seismic isolation layer displacement of 0.35 m is 2.8 s, and the natural period of the seismic isolated building is 3.2 s. The scribble record obtained by the main shock is shown in Fig. 2.

Fig. 5 shows the acceleration waveform recorded by the main shock at KMM004. It is observed that the long-period component appears after 30 s. Fig. 6 shows the displacement response spectrum of the main shock record. It is clear that the component with a period of 3.0 s is predominant. Specifically, a sharp peak can be confirmed in the EW direction at approximately 3.0–4.0 s.

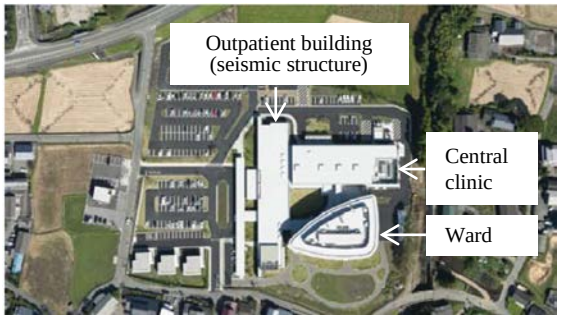

Fig. 3 – Seismic isolated hospital site[3)]

Fig. 4 – Exterior of the ward[3)]

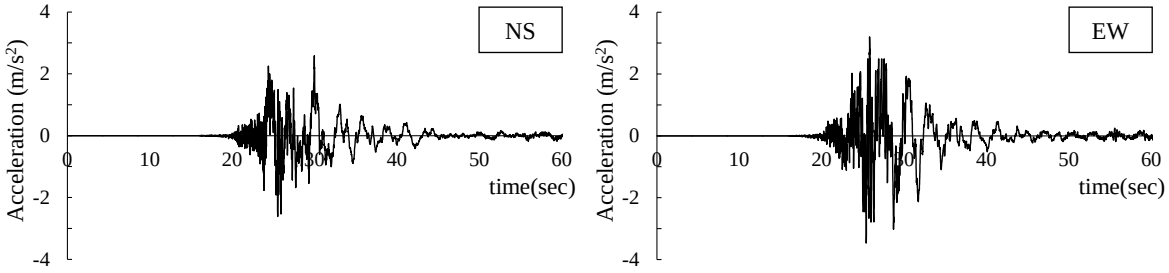

Fig. 5 – Acceleration waveform recorded for the main shock at K-NET Ichinomiya (KMM004)

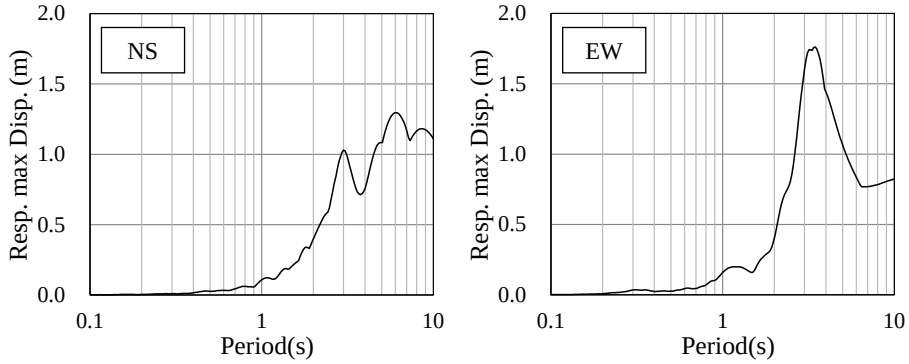

Fig. 6 – Displacement response spectrum of the main shock recorded at K-NET Ichinomiya (KMM004) (h = 0.05)

3. Outline of microtremor array observation

We conducted the microtremor array observation in the range of approximately 3 × 7 km centered at the seismic isolated hospital and KMM004. The observation interval was a 500-m mesh, and the vicinity of both points is a 250-m mesh. The total number of observation points was 147. For the deep strata, we used previous observation results [4, 5] and estimated the S-wave velocity structure of the surface strata on the basis of this observation. The observation equipment used was JU410 (Hakusan Co., Ltd.). As shown in Fig. 7, we conducted a miniature array observation (in which three instruments were evenly arranged at the center and circumference of a circle with a radius of 0.6 m) and an irregular array observation (in which two instruments were arranged at the position of approximately 5 m away from the center of the circle). The observation time was 15 min per point.

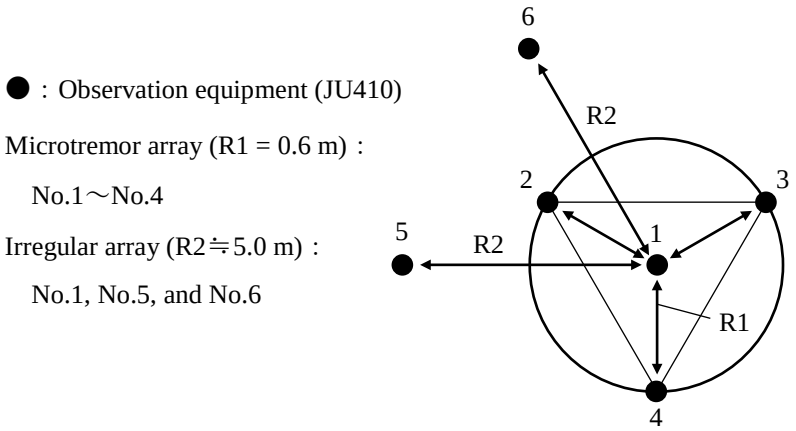

Fig. 7 – Observation equipment layout

4. Analysis results of microtremor observation records

4.1 Outline of the analysis method

(a) Predominant period

To estimate the dominant period, we calculate the power spectrum of each component using the observation record of the equipment placed at the center of the circle to observe the minimal array and calculate the H/V spectrum ratio using Equation (1).

$$H/V\ (\omega) = \frac{\sqrt{NS(\omega) \times EW(\omega)}}{UD(\omega)} \tag{1}$$

where *H/V* (ω) is the H/V spectrum ratio, *NS*(*ω*) is the power spectrum of the NS direction component, *EW*(*ω*) is the power spectrum of the EW direction component, and *UD*(*ω*) is the power spectrum of the UD direction component.

(b) Estimation of the one-dimensional S-wave velocity structure

We analyzed the observation records of the minimal array using the nc-CCA method [6]; the irregular array records were analyzed using the CCA method [7, 8]. First, we conducted the correlation analysis of the observed data by the SPAC method [9] and calculated the dispersion curve of the phase velocity. Next, we repeatedly corrected the surface soil model so that the obtained dispersion curve matched the theoretical dispersion curve, which was calculated assuming the stratified ground, as well as estimated the one-dimensional S-wave velocity structure.

4.2 Predominant period distribution of the ground

Fig. 8 shows the predominant period distribution of the ground. For the surface strata (target period: approximately 0–1.0 s), the short period was dominant in the southwest side, and the long-period was dominant in the northeast side. However, considering the deep strata (target period: 2.0 s or more), the dominant period in the west is longer than that in the east.

Fig. 9 shows the H/V spectrum ratios in the vicinity of the seismic isolated hospital and KMM004. Considering the surface strata, the dominant period was 0.45–0.60 s in the vicinity of the hospital and 0.30–0.45 s in the vicinity of KMM004; thus, the ground at KMM004 was slightly stiffer than that at the hospital. Considering the deep strata, the predominant period was 3.5–4.0 s in the vicinity of the hospital and 2.0–2.5 s in the vicinity of KMM004; thus, the ground was stiffer around KMM004, which differs from the surface strata case.

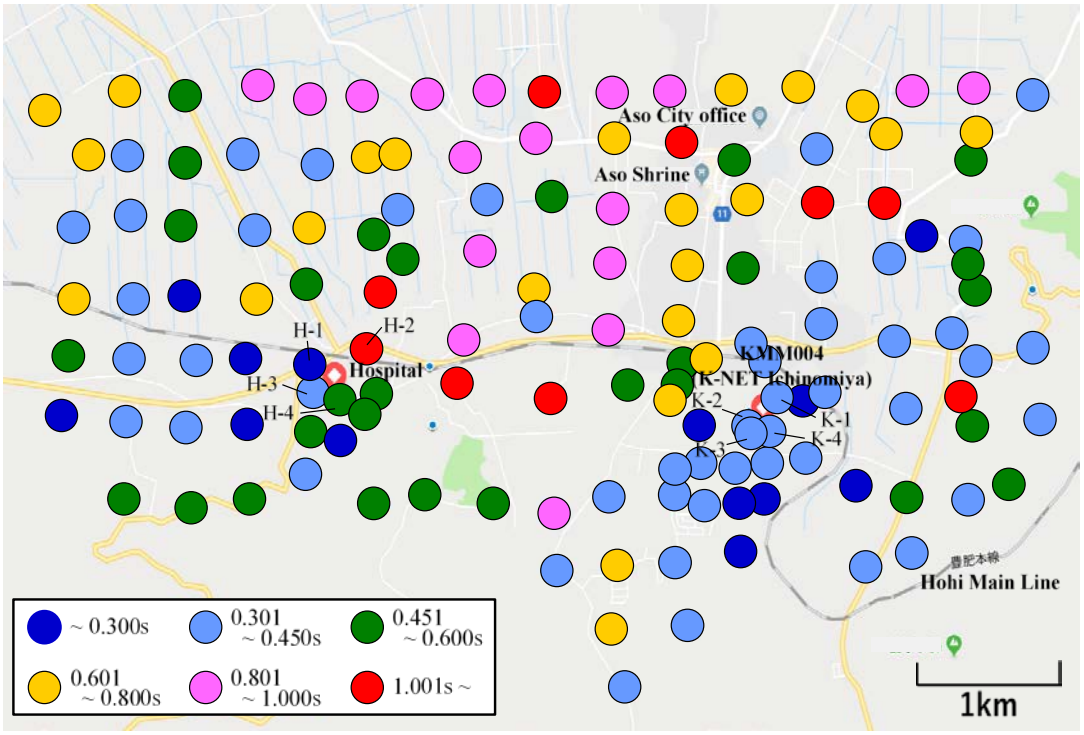

(a) Considering surface strata

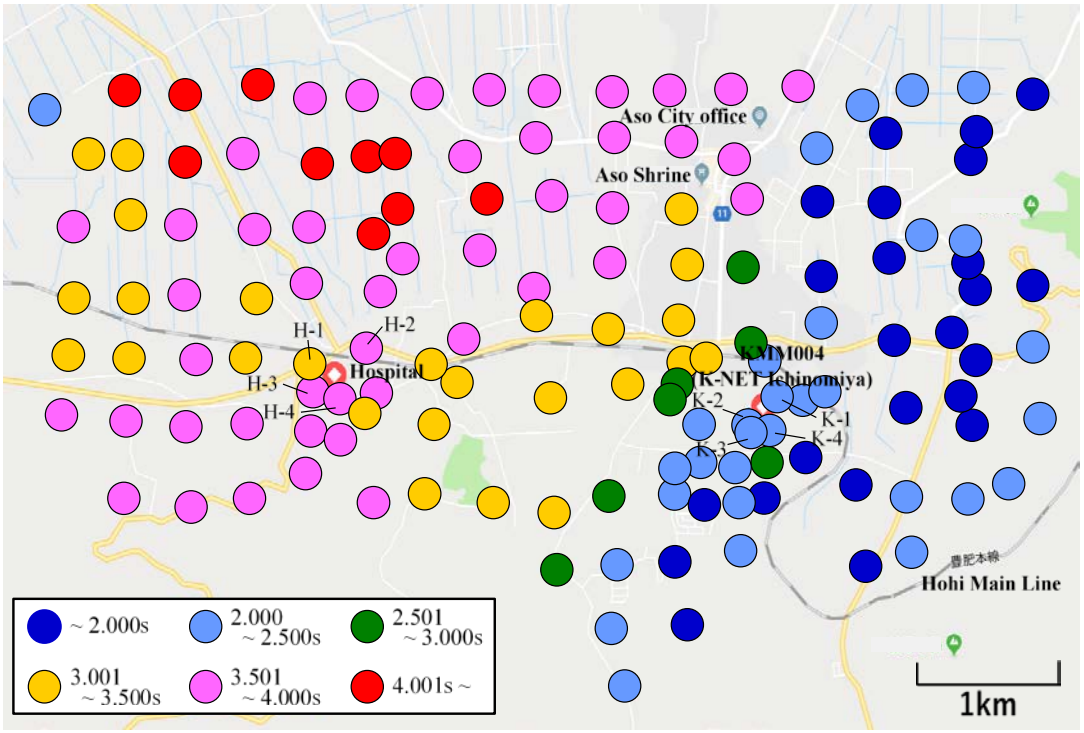

(b) Considering deep strata

Fig. 8 – Predominant period distribution of the ground

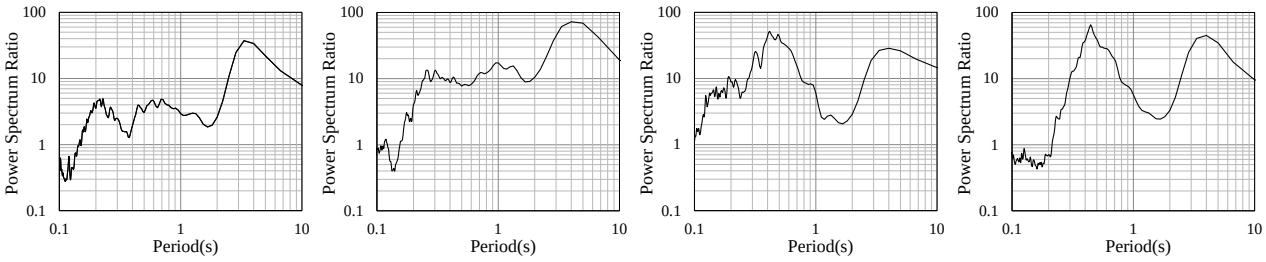

(a) Vicinity of the hospital site (H-1–H-4)

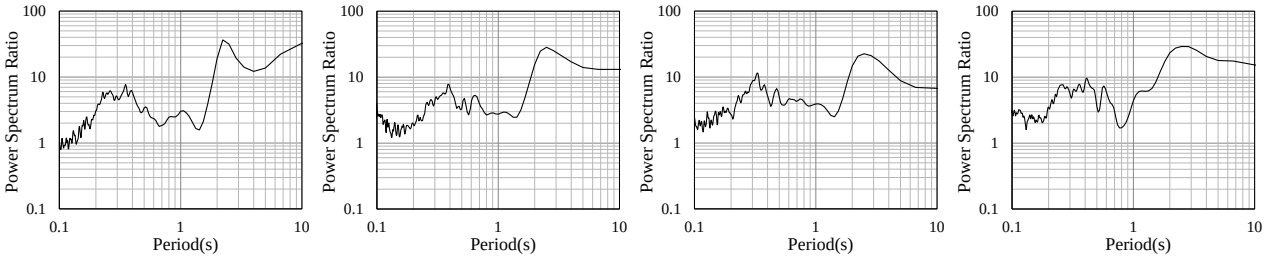

(b) Vicinity of the KMM004 site (K-1–K-4)

Fig. 9 – H/V spectrum ratio

4.3 One-dimensional S-wave velocity structure

Fig. 10 shows the one-dimensional S-wave velocity structure estimated in the vicinity of the hospital and KMM004. The S-wave velocity up to the depth of approximately 30 m is obtained, and the stratum with a relatively large contrast appears at the depth of approximately 10 m in the vicinity of the hospital site and at the depth of approximately 20 m in the vicinity of the KMM004 site.

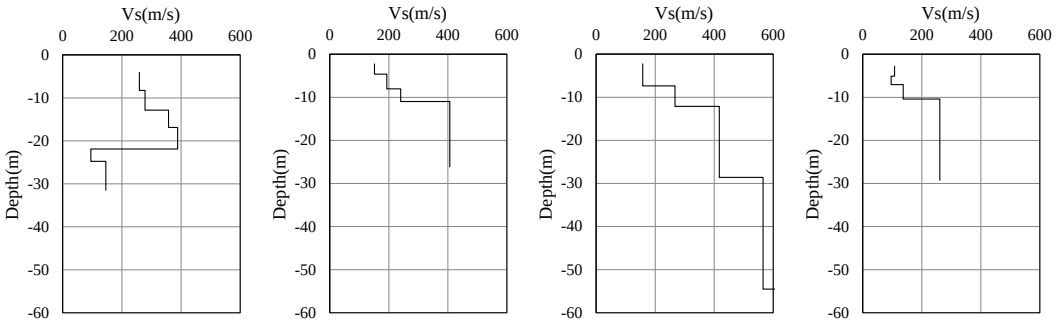

(a) Vicinity of the hospital site (H-1–H-4)

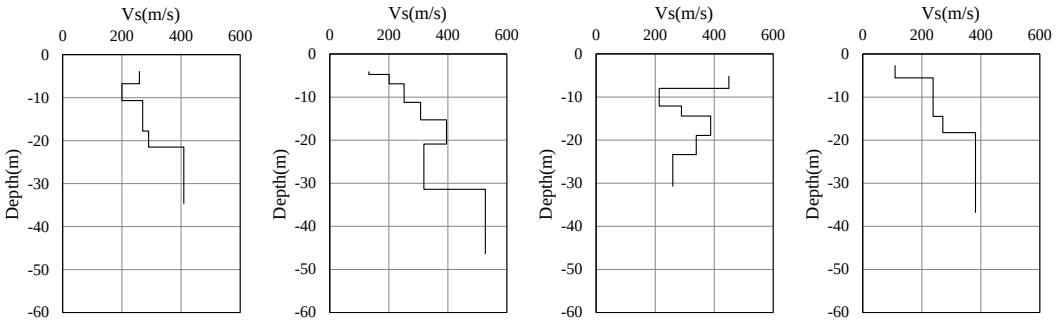

(b) Vicinity of the KMM004 site (K-1–K-4)

Fig. 10 – One-dimensional S-wave velocity structure model

5. Estimation of the ground motion at the seismic isolated hospital site

We create the one-dimensional ground models in the vicinity of the seismic isolated hospital and KMM004 using the S-wave velocity structure that was estimated in the previous section. In architectural engineering, the S-wave velocity is usually modeled above the engineering bedrock of approximately 400 m/s. However, considering that the long-period component of 3.0 s is dominant in the observation records, we modeled the deeper ground, which had the *Vs* value of 1000 m/s. Then, we estimated the ground motion at the hospital site using the following procedure:

[Step1]

We input the observation record of the main shock at KMM004 into the soil structure model surface position of KMM004 and calculate the strong motion at the engineering bedrock by pulling back.

[Step2]

Assuming that the ground motions at the engineering bedrock at both points are the same, we input the pulled-back ground motion into the bottom layer of the hospital ground model.

[Step3]

We calculate the surface response acceleration of the hospital ground model.

We calculated the average S-wave velocity structure that was obtained from the information of the observation points around the target point on the basis of the altitude and created the ground model. We set the soil densities of both points on the basis of the results of the geotechnical investigation conducted in building construction and seismometer installation. Regarding the deep strata property, we used the database of the “Japan Seismic Hazard Information Station” [4] for the hospital model and the previous observational results [5] for the KMM004 model. Therefore, we conducted the analysis using the soil data shown in Table 1. The analysis method is an equivalent linear analysis. The boundary condition was a viscous boundary, and the initial damping factor *h* was 0.02. The nonlinear characteristic (Fig. 11) in the surface strata was obtained from reference number 10, and the deep strata (*Vs* of 500 m/s or more) was linear.

Fig. 12 shows the acceleration waveform of the estimated ground motion. For comparison, the figure also shows the observation record at KMM004. Although the maximum acceleration is approximately the same as that in the observation record, a relatively large difference occurs after 30 s when the long-period component appears. Furthermore, it can be confirmed that in the displacement response spectrum of the estimated ground motion shown in Fig. 13, there is a considerable difference in the long-period component compared with that in the observation record. For the displacement at 3.0 s, which is almost equal to the equivalent period of the seismic isolated hospital, the displacement is approximately 0.28 m in the NS direction and approximately 0.44 m in the EW direction, which is approximately the same as the maximum displacement obtained in the scribble record. Both sites of the seismic isolated hospital and KMM004 have particularly different deep soil structures; it is assumed that this characteristic results in the difference between the ground motions at both points.

Table 1 – Soil property

(a) Hospital ground model

Stratum number	Depth (m)	Density (ton/m^3)	S-wave velocity (m/s)
1	0–3.2	1.07	169
2	−3.2–5.6	1.07	169
3	−5.6–9.4	1.75	193
4	−9.4–12.3	1.32	257
5	−12.3–13.5	1.32	341
6	−13.5–17.7	1.88	341
7	−17.7–23.4	2.06	341
8	−23.4–24.0	2.04	295
9	−24.0–26.8	1.82	295
10	−26.8–42.0	1.82	345
11	−42.0–625	2.09	1100
12	—	2.09	1100

(b) KMM004 ground model

Stratum number	Depth (m)	Density (ton/m^3)	S-wave velocity (m/s)
1	0–0.3	1.54	291
2	−0.3–3.0	1.55	291
3	−3.0–4.0	1.67	291
4	−4.0–5.0	1.73	291
5	−5.0–6.0	1.74	325
6	−6.0–7.0	1.83	325
7	−7.0–8.0	1.77	351
8	−8.0–9.0	1.83	233
9	−9.0–10.0	1.85	233
10	−10.0–11.0	1.93	233
11	−11.0–12.0	2.02	261
12	−12.0–13.0	2.08	298
13	−13.0–14.0	2.12	298
14	−14.0–15.3	2.09	348
15	−15.3–18.9	2.09	392
16	−18.9–20.9	2.09	368
17	−20.9–23.3	2.09	329
18	−23.3–31.4	2.09	298
19	−31.4–141	2.09	527
20	−141–360	2.09	652
21	−360–913	2.09	1117
22	—	2.09	2331

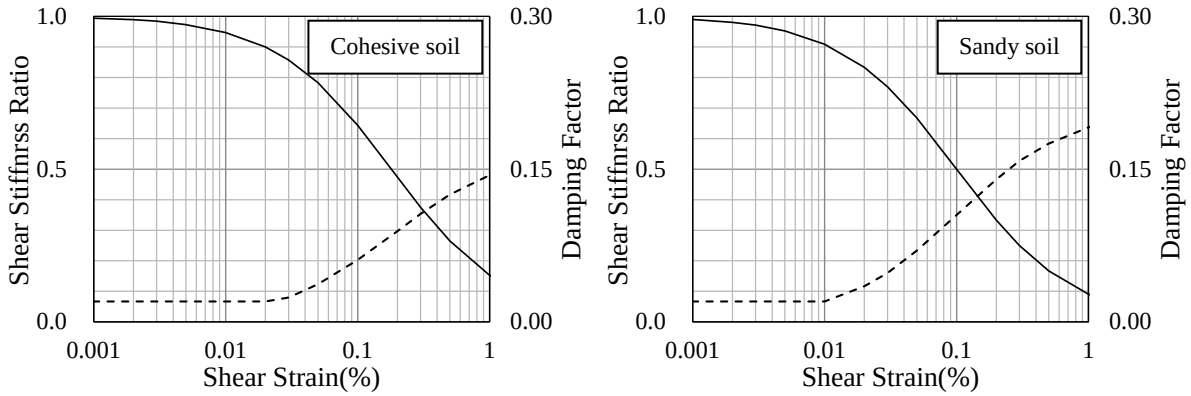

Fig. 11 – Nonlinear characteristic in the surface strata

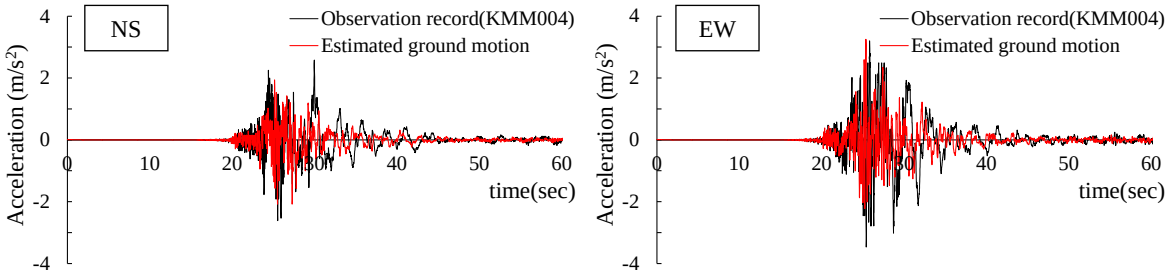

Fig. 12 – Acceleration waveform of the estimated ground motion

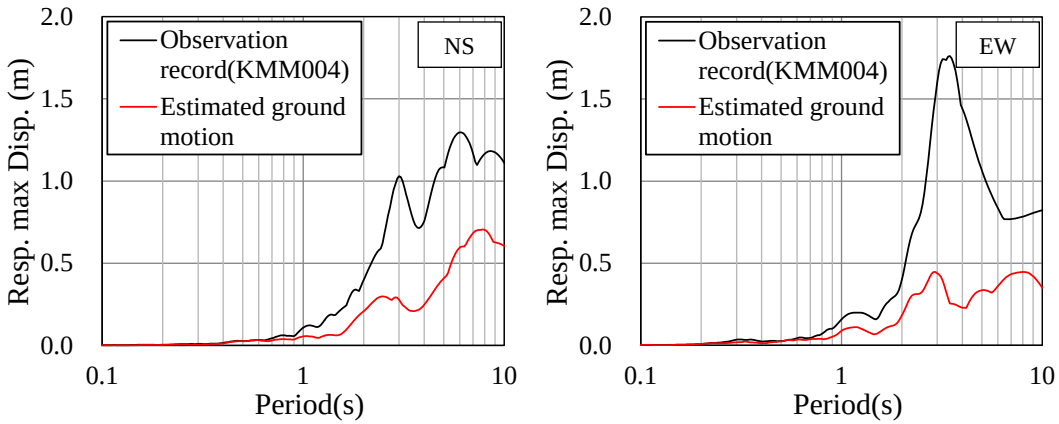

Fig. 13 – Displacement response spectrum of the estimated ground motion (h = 0.05)

6. Conclusions

In this study, we conducted microtremor array observations and estimated the soil structure in the vicinity of the seismic isolated hospital and KMM004, which is a strong motion observation point. In addition, we created one-dimensional ground models considering the deep ground with the S-wave velocity of more than 1000 m/s at both points. In addition, we used the main shock record of the Kumamoto earthquake obtained at KMM004 and estimated the ground motion at the hospital site during the main shock. The following conclusions can be made:

1) Focusing on the surface strata (target period: approximately 0–1.0 s), the dominant period was 0.45–0.60 s in the vicinity of the hospital and 0.30–0.45 s in the vicinity of KMM004; the ground at KMM004 was slightly stiffer than that at the hospital. However, considering the deep strata (target period: 2.0 s or more), the predominant period was 3.5–4.0 s in the vicinity of the hospital and 2.0–2.5 s in the vicinity of KMM004; the ground was stiffer around KMM004, and the tendency was different compared with the case of surface strata.

2) The maximum acceleration of the estimated ground motion at the hospital site was similar to the strong motion record at KMM004; however, the power of the long-period component decreased. By reading the displacement response spectrum value at the period of 3.0 s, which is almost equal to the equivalent period of the seismic isolated hospital, it was determined to be approximately 0.28 m in the NS direction and approximately 0.44 m in the EW direction, which was approximately the same as the maximum displacement obtained in the scribble record.

3) Although the distance between the hospital and KMM004 was not large, because both sites had different deep soil structures, it was assumed that this characteristic resulted in the difference between the ground motions at both points.

7 Acknowledgment

A part of the observation data and analysis tools were provided by the National Research Institute for Earth Science and Disaster Resilience (NIED).

8 References

[1] Research Committee on Earthquake Disaster (2018): Report on the damage investigation of the 2016 Kumamoto earthquakes, architectural institute of Japan, 367-368

[2] Takayama, M. and Morita, K. (2017): A study on the response of seismically isolated hospital in Aso during 2016 Kumamoto earthquake, *Summaries of technical papers of annual meeting Architectural Institute of Japan*, 1051-1052

[3] Yamamoto, H., Tanaka, Y., Yamane, T. and Nakamizo, D. (2017): Seismic isolated structural hospital that maintained the function during the 2016 Kumamoto earthquake [Translated from Japanese.], *12th Japan-China Joint Conference on Structural Engineering*.

[4] National Research Institute for Earth Science and Disaster Resilience: Japan Seismic Hazard Information Station, http://www.j-shis.bosai.go.jp/en/

[5] Kawasaki, I., Gotsu, Y., Uezono, S., Shigehugi, M. and Kanno T. (2018): A study on long period ground motion observed at K-NET Ichinomiya during the 2016 Kumamoto Earthquake, *Summaries of technical papers of annual meeting Architectural Institute of Japan*, 701-702

[6] Tada, T., Cho, I., and Shinozaki, Y. (2007): Beyond the SPAC method: Exploiting the wealth of circular-array methods for microtremor exploration, *Bulletin of the Seismological Society of America*, 97, 2080-2095.

[7] Cho, I., Tada, T., and Shinozaki, Y. (2004): A new method to determine phase velocities of Rayleigh waves from microseisms, *Geophysics*, 69, 1535-1551.

[8] Cho, I., Tada, T., and Shinozaki, Y. (2006): Centerless circular array method: Inferring phase velocities of Rayleigh waves in broad wavelength ranges using microtremor records, *Journal of Geophysical Research*, 111, B09315.

[9] Tada, T., Cho, I., and Shinozaki, Y. (2009): New circular-array microtremor techniques to infer Love-wave phase velocities, *Bulletin of the Seismological Society of America*, 99, 2912-2926.

[10] Koyamada, K., Miyamoto, Y., and Miura, K. (2003): Nonlinear property for surface strata from natural soil samples, *The 38th Japan National Conference on Geotechnical Engineering*.

